Sum-frequency generation from an isotropic chiral medium

Pao-Keng Yang and Jung Y. Huang

Institute of Electro-Optical Engineering, Chiao Tung University, Hsinchu, Taiwan, Republic of China

Received October 31, 1997; revised manuscript received March 6, 1998

We report a theoretical analysis of nonlinear optical sum-frequency generation from the bulk of a chiral liquid in the dipole approximation. In our theoretical formulation the circular birefringence effect of a chiral medium was properly taken into account. The angular dependence of the reflected and transmitted sum-frequency signals on the incident angles of two input beams was calculated to yield the optimal geometry for probing bulk chirality. We also derived a microscopic expression for the totally antisymmetric part of a second-order nonlinear optical susceptibility to elaborate unique features in the studies of chirality-related properties with sum-frequency generation. © 1998 Optical Society of America [S0740-3224(98)01706-8]

OCIS codes: 190.4720, 190.2620, 260.1440.

1. INTRODUCTION

Molecules that cannot be superimposed with their mirror images are called chiral molecules. Two possible configurations, of l and d forms (l is levrotatory and d is dextrorotatory), exist for each molecule. Many biologically and pharmaceutically important molecules have chiral structures. It is interesting to know that, in a typical pharmaceutical process, only one enantiomer will assist the treatment of diseases while the other may lead to counterproductive effects. Chiral segments in a biologically active molecule also play an important role in determining the molecular folding structure. The existence of a chiral purity[1] in living systems remains a major mystery in life science. Inasmuch as optical probes can be applied to any medium that is accessible to light, the development of new optical techniques for investigating chirality-related structures and properties becomes highly desirable. Such techniques will also improve our understanding of many interesting phenomena ranging from a living system to an artificial device made with ferroelectric liquid-crystal materials.[2]

In linear optics, optical rotatory dispersion (ORD) and circular dichroism (CD) are popular markers for probing molecular chirality. The former is based on the difference in the index of refraction between left-hand circularly polarized (LHCP) and right-hand circularly polarized (RHCP) light, whereas the CD technique measures the difference in absorption coefficients between the two kinds of circularly polarized light. These linear optical effects originate from coupling between the magnetic and the electric transition dipole moments in a molecule[3]; therefore the resulting signals are usually weak, with a typical response ($\Delta\varepsilon/\varepsilon$) of 0.1% in a CD measurement.[4] Recently Hicks and co-workers[4–8] successfully extended ORD and CD to surface second-harmonic generation (SHG). The resultant SHG-CD and SHG-ORD techniques, which originate from electric-dipole effects, produce a stronger signal than those from chirality-induced linear optical effects. The normalized difference of the detected SHG intensity with LHCP and with RHCP light was found to be as large as 0.25. Their results also showed that the SHG-CD signal can be deduced from two separately measured SHG spectra with LHCP and RHCP light. Other experiments,[9,10] which measured the SHG intensity difference between two kinds of linearly polarized light, yielded a similar sensitivity to molecular chirality. Owing its high sensitivity and surface specificity, SHG has been considered to be superior to the linear optical techniques for probing the surface chirality in various materials.

Sum-frequency generation (SFG),[11–13] which is also a second-order nonlinear optical process, has been demonstrated to be a useful tool for studying surface and interfacial phenomena with molecular specificity. The sum-frequency signal from an isotropic medium vanishes under the dipole approximation. However, a nonlinear polarization from the electric-dipole transitions can readily be produced inside an isotropic chiral medium, which makes SFG sensitive to bulk chirality.

SFG can be properly described in terms of second-order nonlinear optical susceptibility $\chi^{(2)}_{ijk}$. The totally antisymmetric part ${}^{(A)}\chi^{(2)}_{ijk}$ of the third-rank tensor $\chi^{(2)}_{ijk}$ is defined by

$$ {}^{(A)}\chi^{(2)}_{ijk} = \chi^{(2)}_{a}\varepsilon_{ijk}, \tag{1}$$

where $\chi^{(2)}_{a} \equiv [\varepsilon_{ijk}\chi^{(2)}_{ijk}]/6$, where ε_{ijk} is the Levi-Civita symbol. Owing to the pseudotensor nature of ε_{ijk},[14] $\chi^{(2)}_{a}$ becomes a pseudoscalar that is invariant under rotational transformation but changes sign under mirror reflection. Therefore, in a chiral liquid in which no mirror symmetry exists, the pseudoscalar does not vanish. The theory of SFG from a chiral liquid was described by Giordmaine in 1965.[15] The experimental demonstration was later performed by frequency mixing the fundamental beam from a ruby laser at 694.3 nm with its second harmonic in a

solution of arabinose.[16] The study showed that a transmitted sum-frequency signal generated from a susceptibility pseudoscalar does not vanish only when the nonlinear optical process involved is nondegenerate ($\omega_1 \neq \omega_2$), near resonance, and in a noncollinear beam geometry.

A totally antisymmetric tensor changes sign by exchanging any two indices. For the SHG process ($\omega_1 = \omega_2$) the nonlinear susceptibility is zero because the last two indices of this third-rank tensor commute. Note that Kleinman symmetry[17] must be violated to yield a nonvanishing totally antisymmetric susceptibility, which explains why chirality-induced SFG processes occur only near resonance. In a collinear geometry the induced nonlinear polarization is nearly parallel to the direction of the transmitted sum-frequency beam. An oscillating dipole does not radiate along the dipole direction, so the SFG signal will vanish in a collinear beam configuration.

When an incident beam is refracted into a chiral medium, it splits into two parts with different refractive angles and polarizations. One beam is LHCP and the other is RHCP. This effect is called circular birefringence and can lead to energy coupling between s- and p-polarized waves. Therefore the nonlinear reflection and transmission for s- and p-polarized waves in a chiral medium cannot be solved separately. Some researchers have studied SFG reflection from a chiral medium by ignoring the circular birefringence effect.[18,19] In this paper we include circular birefringence in our formalism to yield a more-accurate description. As far as SFG-CD and SFG-ORD are concerned, it is also important to estimate the nonlinear optical response from the bulk of a chiral medium. Our theoretical formalism enables us to design an optimum experimental geometry for SFG-CD and SFG-ORD. Our results also show that the surface sum-frequency signal can be distinguished from that from bulk with an appropriate polarization combination of the input and output beams.

This paper is organized as follows: Section 2 outlines the calculation procedure for the reflected and the transmitted sum-frequency signals from a chiral liquid. The chirality-induced nonlinear polarizations are then described. We then derive a microscopic expression for the totally antisymmetric part of a second-order nonlinear optical susceptibility. Some numerical results and discussion are presented in Section 3. Finally, some conclusions are drawn in Section 4.

2. BASIC THEORY

A. Solutions of Nonlinear Reflection and Transmission

In the following discussion, LHCP light will be indicated by + and RHCP by − in the subscript of a vector. The polarization basis vectors for the LHCP and RHCP waves are $\hat{e}_{\pm} = (1/\sqrt{2})(\hat{s} \pm i\hat{p})$, where $\hat{s} = \hat{y}$ and $\hat{p} = \hat{k} \times \hat{s}$ and $\hat{k}$ is the unit vector of the wave vector depicted in Fig. 1. For SFG with noncollinear geometry (see Fig. 2), two beams, of frequencies ω_1 and ω_2, are incident upon a semi-infinite chiral medium at incident angles of θ_{1i} and θ_{2i}. After refraction, each beam splits into two circularly polarized waves with different angles of refraction. Four possible combinations of the wave vectors can be chosen to generate the nonlinear polarization; they are

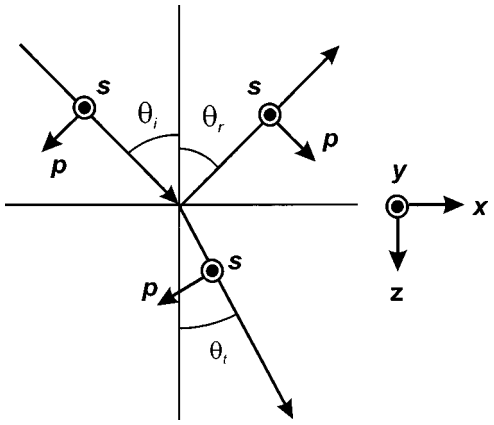

Fig. 1. Schematic showing the s- and p-polarized directions and the propagation directions of the incident, refracted, and reflected waves.

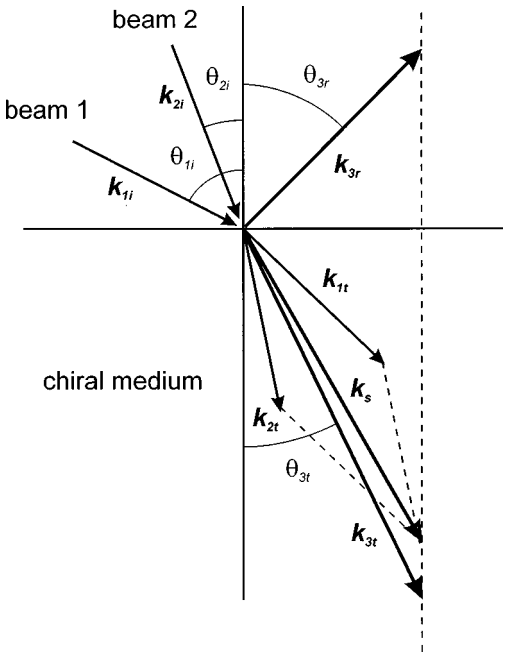

Fig. 2. Vector diagram showing the relative orientations of the wave vectors for the incident, reflected, and refracted waves and the nonlinear polarization source. The splitting of the refracted wave vector by circular birefringence is neglected.

$$\mathbf{k}_{s,1} = \mathbf{k}_{1t+} + \mathbf{k}_{2t+},$$
$$\mathbf{k}_{s,2} = \mathbf{k}_{1t+} + \mathbf{k}_{2t-},$$
$$\mathbf{k}_{s,3} = \mathbf{k}_{1t-} + \mathbf{k}_{2t+},$$
$$\mathbf{k}_{s,4} = \mathbf{k}_{1t-} + \mathbf{k}_{2t-}. \quad (2)$$

The total nonlinear polarization can be expressed as

$$\mathbf{P}^{(2)}(\omega_3 = \omega_1 + \omega_2) = \sum_{j=1}^{4} \mathbf{P}_j^{(2)} = \sum_{j=1}^{4} \mathbf{p}_j^{(2)} \exp[i(\mathbf{k}_{s,j} \cdot \mathbf{r} - \omega_3 t)]. \quad (3)$$

Note that angles of reflection and refraction for each beam can be determined from the nonlinear Snell's law:

$$k_{1i}\sin\theta_{1i} + k_{2i}\sin\theta_{2i} = k_{3r}\sin\theta_{3r} = k_{3t+}\sin\theta_{3t+} = k_{3t-}\sin\theta_{3t-} = k_{s,j}\sin\theta_{s,j} = k_{1t\pm}\sin\theta_{1t\pm} + k_{2t\pm}\sin\theta_{2t\pm} = k_{1t\pm}\sin\theta_{1t\pm} + k_{2t\mp}\sin\theta_{2t\mp}. \tag{4}$$

Chirality is introduced into our theory through the constitutive relations[20]

$$\mathbf{D} = \varepsilon\mathbf{E} + i\xi_c\mathbf{B},$$

$$\mathbf{H} = \mathbf{B}/\mu + i\xi_c\mathbf{E}, \tag{5}$$

where ε, μ, and ξ_c are, respectively, the dielectric constant, permeability, and chirality admittance of the chiral medium. By substituting the constitutive relations into the Maxwell equations we obtain the following two equations:

$$\nabla\cdot[\mathbf{E}(\omega_3) + 4\pi\mathbf{P}^{(1)} + 4\pi\mathbf{P}^{(2)}_{j,\parallel}] = 0 \tag{6}$$

$$\nabla\times\nabla\times\mathbf{E}(\omega_3) - 2\omega_3\mu\xi_c(\omega_3)\nabla\times\mathbf{E}(\omega_3) - \omega_3^2\mu\varepsilon\mathbf{E}(\omega_3) = \frac{4\pi\omega_3^2}{c^2}\mathbf{P}^{(2)}_{j,\pm}, \tag{7}$$

where $\mathbf{P}^{(2)}_{j,\parallel}$ indicates the component of $\mathbf{P}^{(2)}_j$ along $\mathbf{k}_{s,j}$; $\mathbf{P}^{(2)}_{j,+}$ and $\mathbf{P}^{(2)}_{j,-}$ represent the projections of $\mathbf{P}^{(2)}_j$ onto the RHCP and LHCP waves with a wave vector of $\mathbf{k}_{s,j}$. Equation (6) determines the longitudinal part of the sum-frequency amplitude, and Eq. (7) governs the wave propagation of the transverse components with $\mathbf{P}^{(2)}_{j,\pm}$ as the driving source. The general solution of Eqs. (6) and (7) can be expressed as a summation of the homogeneous solution and a particular solution. The homogeneous solution can be written as

$$\mathbf{E}_h = E_{3t+}\hat{e}_{3t+}\exp[i(\mathbf{k}_{3t+}\cdot\mathbf{r} - \omega_3 t)] + E_{3t-}\hat{e}_{3t-}\exp[i(\mathbf{k}_{3t-}\cdot\mathbf{r} - \omega_3 t)]. \tag{8}$$

Here $k_{3t\pm} = k_{3t}(\pm\bar{\xi}_c + \sqrt{1+\bar{\xi}_c^2}) = n_\pm(\omega_3/c)$, with $\bar{\xi}_c = \xi_c(\omega_3)\sqrt{\mu/\varepsilon(\omega_3)}$ and $k_{3t} = (\omega_3/c)\sqrt{\mu\varepsilon(\omega_3)}$. Note that $n_+n_- = \mu\varepsilon(\omega_3)$. E_{3t+} and E_{3t-} are two constants that can be determined with the boundary conditions. We can further decompose the jth nonlinear polarization in terms of the three orthogonal basis vectors, $\hat{e}_{j,+}$, $\hat{e}_{j,-}$, and $\hat{k}_{s,j}$:

$$\mathbf{P}^{(2)}_j = (p_{j,+}\hat{e}_{j,+} + p_{j,-}\hat{e}_{j,-} + \mathbf{p}_{j,\parallel}\hat{k}_{s,j})\times\exp[i(\mathbf{k}_{s,j}\cdot\mathbf{r} - \omega_3 t)], \tag{9}$$

and then a particular solution is found to be

$$\mathbf{E}_{\text{par}} = \left[\frac{4\pi\omega_3^2 p_{j,+}}{c^2(k_{s,j}^2 - 2\bar{\xi}_c k_{s,j}k_{3t} - k_{3t}^2)}\hat{e}_{j,+} + \frac{4\pi\omega_3^2 p_{j,-}}{c^2(k_{s,j}^2 + 2\bar{\xi}_c k_{s,j}k_{3t} - k_{3t}^2)}\hat{e}_{j,-} - \frac{4\pi p_{j,\parallel}}{\varepsilon(\omega_3)}\hat{k}_{s,j}\right]\times\exp[i(\mathbf{k}_{s,j}\cdot\mathbf{r} - \omega_3 t)]. \tag{10}$$

Equation (10) shows that the transverse and the longitudinal fields have different proportional constants with respect to the nonlinear polarization. The inclusion of chirality ($\bar{\xi}_c \neq 0$) also introduces a small difference in the proportional constants between the two transverse field components. Neglect of the difference in the proportions of the nonlinear optical polarization between the transverse and the longitudinal fields had led to inaccurate results in previous publications.[18,19]

We express the reflected sum-frequency field as

$$\mathbf{E}_{3r} = E_{3rs}\hat{e}_{3rs}\exp[i(\mathbf{k}_{3r}\cdot\mathbf{r} - \omega_3 t)] + E_{3rp}\hat{e}_{3rp}\exp[i(\mathbf{k}_{3r}\cdot\mathbf{r} - \omega_3 t)] \tag{11}$$

and then apply the continuity condition to the tangential electric and magnetic fields across the planar boundary. This procedure leads to four equations with which the four unknown parameters, E_{3t+}, E_{3t-}, E_{3rs}, and E_{3rp}, can be determined. These four equations can be written in a compact matrix form:

$$\begin{bmatrix} 1 & 0 & \frac{-1}{\sqrt{2}} & \frac{-1}{\sqrt{2}} \\ 0 & \cos\theta_{3r} & \frac{i}{\sqrt{2}}\cos\theta_{3t+} & \frac{-i}{\sqrt{2}}\cos\theta_{3t-} \\ 0 & -k_{3r} & \frac{i}{\sqrt{2}}k_{3t+} & \frac{-i}{\sqrt{2}}k_{3t-} \\ k_{3r}\cos\theta_{3r} & 0 & \frac{1}{\sqrt{2}}k_{3t+}\cos\theta_{3t+} & \frac{1}{\sqrt{2}}k_{3t-}\cos\theta_{3t-} \end{bmatrix}\begin{bmatrix} E_{3rs} \\ E_{3rp} \\ E_{3t+} \\ E_{3t-} \end{bmatrix} = \sum_{j=1}^{4}\begin{bmatrix} -S_{1,j} \\ S_{2,j}\cos\theta_{s,j} + S_{3,j}\sin\theta_{s,j} \\ k_{s,j}S_{2,j} \\ k_{s,j}S_{1,j}\cos\theta_{s,j} + i\xi_c(\omega_3)\frac{\omega_3}{c}S_{4,j} \end{bmatrix}, \tag{12}$$

where

$$S_{1,j} = \frac{-1}{\sqrt{2}}\left[\frac{4\pi\omega_3^2 p_{j,+}}{c^2(k_{s,j}^2 - 2\bar{\xi}_c k_{s,j}k_{3t} - k_{3t}^2)} + \frac{4\pi\omega_3^2 p_{j,-}}{c^2(k_{s,j}^2 + 2\bar{\xi}_c k_{s,j}k_{3t} - k_{3t}^2)}\right],$$

$$S_{2,j} = \frac{-i}{\sqrt{2}}\left[\frac{4\pi\omega_3^2 p_{j,+}}{c^2(k_{s,j}^2 - 2\bar{\xi}_c k_{s,j} k_{3t} - k_{3t}^2)} - \frac{4\pi\omega_3^2 p_{j,-}}{c^2(k_{s,j}^2 + 2\bar{\xi}_c k_{s,j} k_{3t} - k_{3t}^2)}\right],$$

$$S_{3,j} = \frac{4\pi p_{j,\parallel}}{\varepsilon(\omega_3)},$$

$$S_{4,j} = S_{2,j}\cos\theta_{s,j} + S_{3,j}\sin\theta_{s,j}. \tag{13}$$

We can then solve Eq. (12) to determine the reflected and the transmitted SFG amplitudes.

B. Calculation of the Nonlinear Polarization of a Chiral Liquid

For an isotropic chiral medium, the second-order nonlinear susceptibility tensor possesses six nonvanishing components. In a laboratory coordinate (x, y, z) system (see Fig. 1) these components are related to one another by a single independent parameter, $\chi_a^{(2)}$:

$$\chi_a^{(2)} = \chi_{xyz}^{(2)} = \chi_{yzx}^{(2)} = \chi_{zxy}^{(2)} = -\chi_{xzy}^{(2)} = -\chi_{yxz}^{(2)} = -\chi_{zyx}^{(2)}. \tag{14}$$

The transmitted electric-field amplitudes in the medium can be expressed as

$$\mathbf{E}_{1t} = E_{1ts}\hat{e}_{1ts} + E_{1tp}\hat{e}_{1tp},$$

$$\mathbf{E}_{2t} = E_{2ts}\hat{e}_{2ts} + E_{2tp}\hat{e}_{2tp}. \tag{15}$$

The transmitted field amplitudes are related to the incident fields by means of the Fresnel coefficients,[21] which are described in more detail in Appendix A. Assuming that the refractive angles of the ω_1 and ω_2 beams are θ_{1t} and θ_{2t}, respectively, we can determine the x, y, and z components of the induced nonlinear polarization:

$$p_x^{(2)} = \chi_a^{(2)}(E_{1ts}E_{2tp}\sin\theta_{2t} - E_{1tp}E_{2ts}\sin\theta_{1t}),$$

$$p_y^{(2)} = \chi_a^{(2)}E_{1tp}E_{2tp}\sin(\theta_{2t} - \theta_{1t}),$$

$$p_z^{(2)} = \chi_a^{(2)}(-E_{1tp}E_{2ts}\cos\theta_{1t} + E_{1ts}E_{2tp}\cos\theta_{2t}). \tag{16}$$

The four nonlinear polarization terms in Eq. (3) can be generated with appropriate polarization combinations as the input fields in Eqs. (16). For example, by substituting $(E_{1ts}, E_{1tp}) = (1/\sqrt{2}, i/\sqrt{2})E_{1t+}$ and $(E_{2ts}, E_{2tp}) = (1/\sqrt{2}, i/\sqrt{2})E_{2t+}$ into Eqs. (16), we can deduce the x, y and z components of $\mathbf{p}_1^{(2)}$. The parameters that we need to describe a SFG process are optical frequencies (ω_1, ω_2), incident angles $(\theta_{1i}, \theta_{2i})$, incident field amplitudes (E_{1is}, E_{1ip}) and (E_{2is}, E_{2ip}) of the ω_1 and ω_2 beams, refractive indices $[n_\pm(\omega_1), n_\pm(\omega_2), n_\pm(\omega_3)]$, and the value of the totally antisymmetric part of the second-order susceptibility $\chi_a^{(2)}$. Note that in Eqs. (16) $\chi_a^{(2)}$ can be factored out of the expression for the nonlinear polarization. It is therefore useful to define a normalized intensity by dividing the sum-frequency intensity by $|\chi_a^{(2)}|^2$. The resulting normalized sum-frequency intensity depends only on the linear optical properties of the chiral medium.

C. Microscopic Description of $\chi_a^{(2)}$

The expression for second-order nonlinear polarizability can be derived from the density matrix formalism[22] and was found to contain eight terms. In terms of molecule-fixed Cartesian coordinates (ξ, η, ζ) these terms can be written as

$$\begin{aligned}\alpha_{\xi\eta\zeta}^{(2)}(\omega = \omega_1 + \omega_2) = -\frac{e^3}{\hbar^2}\sum_{g,n,n'}\Bigg[&\frac{(r_\xi)_{gn}(r_\eta)_{nn'}(r_\zeta)_{n'g}}{(\omega - \omega_{ng} + i\Gamma_{ng})(\omega_2 - \omega_{n'g} + i\Gamma_{n'g})} \\ &+ \frac{(r_\xi)_{gn}(r_\eta)_{nn'}(r_\zeta)_{n'g}}{(\omega - \omega_{ng} + i\Gamma_{ng})(\omega_1 - \omega_{n'g} + i\Gamma_{n'g})} \\ &+ \frac{(r_\xi)_{gn'}(r_\eta)_{n'n}(r_\zeta)_{ng}}{(\omega + \omega_{ng} + i\Gamma_{ng})(\omega_2 + \omega_{n'g} + i\Gamma_{n'g})} \\ &+ \frac{(r_\xi)_{gn'}(r_\eta)_{n'n}(r_\zeta)_{ng}}{(\omega + \omega_{ng} + i\Gamma_{ng})(\omega_1 + \omega_{n'g} + i\Gamma_{n'g})} \\ &- \frac{(r_\xi)_{ng}(r_\eta)_{n'n}(r_\zeta)_{gn'}}{(\omega - \omega_{nn'} + i\Gamma_{nn'})}\left(\frac{1}{\omega_2 + \omega_{n'g} + i\Gamma_{n'g}} + \frac{1}{\omega_1 - \omega_{ng} + i\Gamma_{ng}}\right) \\ &- \frac{(r_\xi)_{ng}(r_\eta)_{n'n}(r_\zeta)_{gn'}}{(\omega - \omega_{nn'} + i\Gamma_{nn'})}\left(\frac{1}{\omega_2 - \omega_{ng} + i\Gamma_{ng}} + \frac{1}{\omega_1 + \omega_{n'g} + i\Gamma_{n'g}}\right)\Bigg]\rho_g^{(0)}.\end{aligned} \tag{17}$$

By transforming the molecular-fixed frame into a system of laboratory coordinates (i, j, k) we found that

$$\chi_a^{(2)} = \frac{1}{6}\varepsilon_{ijk}\chi_{ijk}^{(2)} = N\left\langle\frac{1}{6}\varepsilon_{\xi\eta\zeta}\alpha_{\xi\eta\zeta}^{(2)}\right\rangle = N\frac{1}{6}\varepsilon_{\xi\eta\zeta}\alpha_{\xi\eta\zeta}^{(2)} = N\alpha_a^{(2)}, \tag{18}$$

where N denotes the molecular density and $\langle\,\rangle$ is the orientational average of the quantity contained within, over a random distribution. The orientational average in Eq. (18) can be removed because the contraction of $\varepsilon_{\xi\eta\zeta}$ and $\alpha_{\xi\eta\zeta}^{(2)}$ is invariant under the rotational transformation. By substituting the expression for $\alpha_{\xi\eta\zeta}^{(2)}$ in Eq. (17) into Eq. (18) we can write $\chi_a^{(2)}$ as

$$\chi_a^{(2)}(\omega = \omega_1 + \omega_2) = -N \frac{1}{6\hbar^2} \sum_{g,n,n'} \left[\frac{\boldsymbol{\mu}_{gn} \cdot (\boldsymbol{\mu}_{nn'} \times \boldsymbol{\mu}_{n'g})}{(\omega - \omega_{ng} + i\Gamma_{ng})(\omega_2 - \omega_{n'g} + i\Gamma_{n'g})(\omega_1 - \omega_{n'g} + i\Gamma_{n'g})} \right.$$
$$- \frac{\boldsymbol{\mu}_{gn'} \cdot (\boldsymbol{\mu}_{n'n} \times \boldsymbol{\mu}_{ng})}{(\omega + \omega_{ng} + i\Gamma_{ng})(\omega_2 + \omega_{n'g} + i\Gamma_{n'g})(\omega_1 + \omega_{n'g} + i\Gamma_{n'g})}$$
$$+ \frac{\boldsymbol{\mu}_{ng} \cdot (\boldsymbol{\mu}_{n'n} \times \boldsymbol{\mu}_{gn'})}{(\omega - \omega_{nn'} + i\Gamma_{nn'})(\omega_2 + \omega_{n'g} + i\Gamma_{n'g})(\omega_1 + \omega_{n'g} + i\Gamma_{n'g})}$$
$$\left. - \frac{\boldsymbol{\mu}_{ng} \cdot (\boldsymbol{\mu}_{n'n} \times \boldsymbol{\mu}_{gn'})}{(\omega - \omega_{nn'} + i\Gamma_{nn'})(\omega_1 - \omega_{ng} + i\Gamma_{ng})(\omega_2 - \omega_{ng} + i\Gamma_{ng})} \right] (\omega_1 - \omega_2)\rho_g^{(0)}. \quad (19)$$

The important feature of $\chi_a^{(2)} \propto (\omega_1 - \omega_2)$ from Eq. (19) allows us to conclude that there should be no second-harmonic signal from $\chi_a^{(2)}$ because $\chi_a^{(2)} = 0$ as $\omega_1 = \omega_2$. Furthermore, from Eq. (19) we find that the totally antisymmetric part is proportional to the scalar triple product of the three successive transition dipole moments [i.e., $\chi_a^{(2)} \propto \boldsymbol{\mu}_{gn} \cdot (\boldsymbol{\mu}_{nn'} \times \boldsymbol{\mu}_{n'g})$] that are involved in a three-photon process. To yield a nonvanishing $\chi_a^{(2)}$, the three successive transition dipole moments must not be coplanar; the molecule should therefore possess stereostructures. Note that $\boldsymbol{\mu}_{nn'} \times \boldsymbol{\mu}_{n'g}$ exhibits the transformation property of an axial vector. Therefore the inner product of a polar vector μ_{gn} and the axial vector $\boldsymbol{\mu}_{nn'} \times \boldsymbol{\mu}_{n'g}$ generates a pseudoscalar that changes sign under mirror reflection, which explains why $\chi_a^{(2)}$ can sensitively reflect molecular chirality.

3. NUMERICAL RESULTS AND DISCUSSION

The first SFG measurement with a 2.46-M solution of arabinose[16] showed that the magnitude of $\chi_a^{(2)}$ is $\sim 1 \times 10^{-10}$ esu. With the known number density of molecules, the chirality-induced nonlinear polarizability $\alpha_a^{(2)}$ is estimated to be 1×10^{-31} esu, which is approximately 5% of a typical achiral nonlinear polarizability component $\alpha_{\xi\xi\xi}^{(2)}$.[23]

In a non-phase-matching three-wave-mixing process the effective interaction length is limited mainly by the coherence length. Inasmuch as the coherence length l_c in a liquid is $\sim 1 \times 10^{-3}$ cm, the value of $\chi_a^{(2)} l_c$ can be as large as 1×10^{-13} esu. With a detectability of $\chi^{(2)} l_c \approx 1 \times 10^{-17}$ esu in a typical detection system, we conclude that submicromolar chiral concentration should be detectable by SFG. Note that we can further verify the sum-frequency signal from bulk chirality with an observation of a vanishing signal from a racemic mixture. The absorption of a chiral medium may reduce the value of the effective interaction length. We can take the absorptive effect at frequency ω_j into account in our formalism by introducing complex wave vectors $k_{jt\pm} \rightarrow k'_{jt\pm} + i\beta_{j\pm}$ in Eqs. (2) and (8), where $\beta_{j\pm}$ is the attenuation coefficient at frequency ω_j with polarization along $\hat{e}_\pm$. For a strongly absorptive medium the effective interaction can be reduced to $1/\beta$.

A. Numerical Results

In Fig. 3 the reflected and transmitted SFG signals are plotted as a function of the incident angle of beam 1 with three different polarization combinations of the two input beams. The incident angle of beam 2 was fixed at 40°. Here sp denotes that input beam 1 is s polarized and beam 2 is p polarized. The frequencies and the refractive indices used in the calculations are $\omega_1 = 10\,000$ cm^{-1}, $\omega_2 = 20\,000$ cm^{-1}, and $(n_{1\pm}, n_{2\pm}, n_{3\pm}) = (1.38, 1.40, 1.43)$. We first neglect the circular birefringence of the chiral liquid. The resulting SFG signals with three polarization combinations of pp, sp, and ps are shown in Fig. 3 by dotted, solid, and dashed curves, respectively. Owing to the vanishing intensity, we do not present the sum-frequency signal with an ss polarization combination in Fig. 3. All SFG intensities have been normalized to $|\chi_a^{(2)}|^2 |E_{1i}|^2 |E_{2i}|^2$. The polarization combinations of sp and ps generate a p-polarized SFG signal in the reflected and the transmitted directions, whereas the pp polarization combination generates an s-polarized signal. It is interesting to note that, in a collinear beam geometry ($\theta_{1i} = \theta_{2i} \cong 40°$), the transmitted SFG signal vanishes for all polarization combinations, whereas at

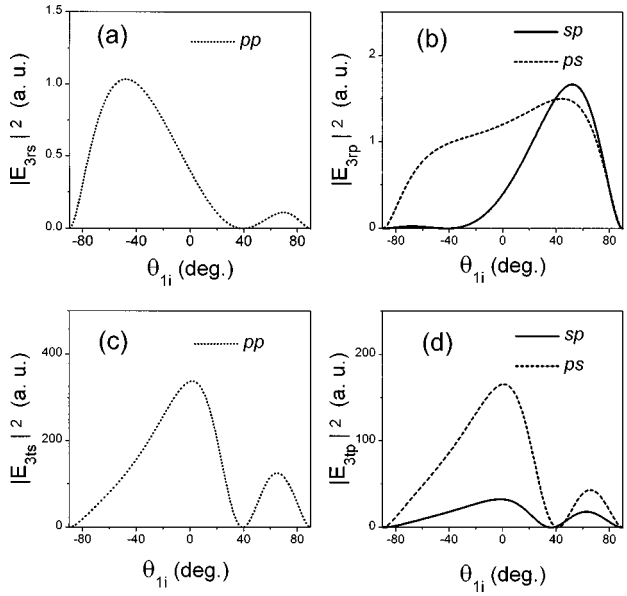

Fig. 3. Calculated sum-frequency intensities [(a), (b) in reflection; (c), (d) in transmission] plotted as a function of the incident angle of input beam 1. In the calculations, the incident angle of beam 2 was fixed at 40°. Left, the input polarizations for two input beams are p polarized. Right, the curves are generated with ps (p for beam 1 and s for beam 2) or sp input polarization combinations. The circular birefringence of the material is neglected.

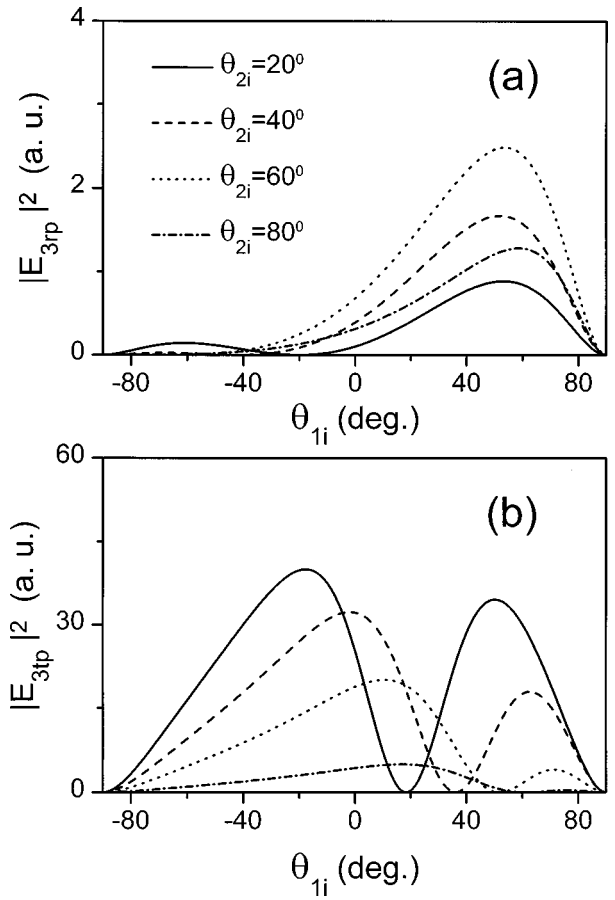

Fig. 4. (a) Reflected sum-frequency signal with sp input polarization combination plotted as a function of the incident angle of beam 1. The incident angle of beam 2 is increased as shown. (b) Similar results for the transmitted sum-frequency signal.

this incident angle the reflected SFG signal with the sp- and ps-polarization combinations achieves a maximal value. This result indicates that the noncollinear requirement can be eliminated in an oblique-incidence configuration if the reflected SFG signal is detected.

In Fig. 4(a) the reflected SFG signal is plotted as a function of the incident angle of beam 1 with the incident angle of beam 2 varying from 20° to 80°. The sp polarization combination was chosen in the calculations. The maximum reflected SFG signal first increases when the incident angle of the beam 2 is increased from $\theta_{2i} = 20°$ to $\theta_{2i} = 60°$ and then decreases when θ_{2i} is increased further. The decrease of the SFG peak intensity at $\theta_{2i} = 80°$ can be ascribed to the effect of the reduced transmissivity at the grazing incidence, in which only a small portion of incident light is refracted into the chiral medium to induce the nonlinear polarization. Therefore there exists optimum incident angles for beams 1 and 2 to generate a maximal reflected SFG signal. Detailed analyses show that the maximum SFG intensity can be achieved with the incident angle of beam 1 fixed at 54° and that of beam 2 fixed at 63°.

In Fig. 4(b) the transmitted SFG signal is plotted. The maximal SFG signal decreases as θ_{2i} increases from 20° to 80°. The transmitted intensity vanishes at the collinear geometry. Further analyses show that the maximal signal can be achieved with the s-polarized wave (beam 1) incident at $\theta_{2i} = 0°$, whereas the p-polarized wave (beam 2) is incident near the Brewster angle.

The reflected SFG intensity depends both on the magnitude of the nonlinear polarization and on the angle between the nonlinear polarization and the reflected direction of the SFG signal. The nonlinear polarization generated from a chiral liquid is proportional to the cross product of the two transmitted fields of two input beams [$\mathbf{P}^{(2)} = \chi_a^{(2)}\mathbf{E}_{1t} \times \mathbf{E}_{2t}$]. The transmitted Fresnel coefficients for both s- and p-polarized light are monotonically decreasing functions of the incident angle. Thus the product of the s- and the p-polarized transmitted fields reaches a maximum at normal incidence. The dependence of the reflected SFG signal on the angle between the nonlinear polarization and the propagation direction of the reflected SFG signal suggests that the SFG intensity should reach a maximum when this angle is 90°. This condition can be attained with two input beams both incident at the Brewster angle, which has a value of 54.5° for the medium considered here. The optimal incident angles that we found above for two input beams to generate the maximum reflected SFG signal are close to the Brewster angle. This result suggests that the angle between the nonlinear polarization and the propagation di-

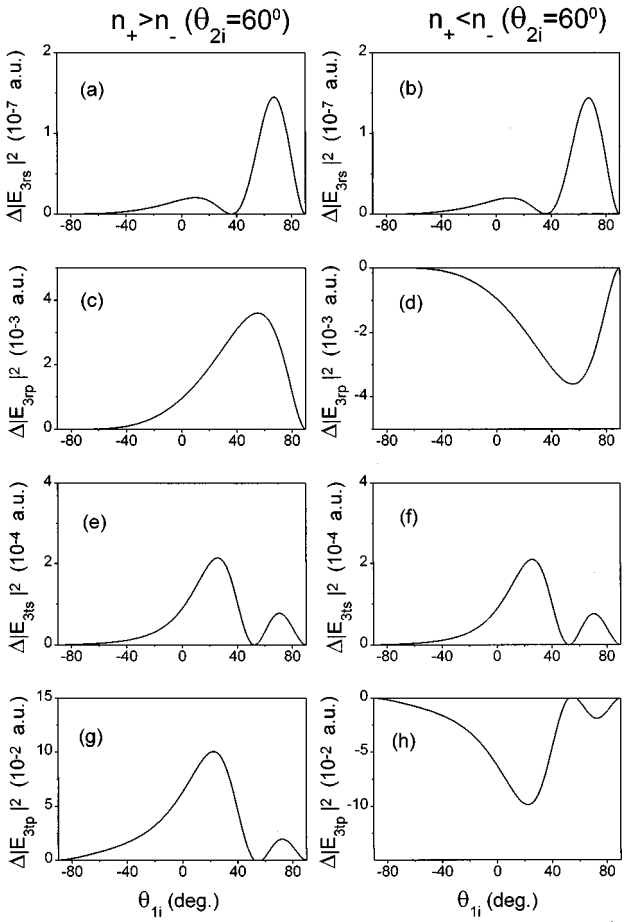

Fig. 5. Calculated SFG intensity corrections for the circular birefringence of material. The dotted curves shown in Fig. 4 with $\theta_{2i} = 60°$ and a vanishing circular birefringence were chosen for the intensity references. The corrections for $n_+ > n_-$ are shown at the left; at the right the corrections for $n_+ < n_-$ are presented.

rection of the reflected SFG signal play a crucial role in determining the magnitude of the reflected SFG signal.

Figure 5 shows the SFG intensity corrections caused by the circular birefringence effect of a chiral medium. The dotted curves in Fig. 4 with $\theta_{2i} = 60°$ are used for the intensity references without circular birefringence. The intensity corrections with $n_+ > n_-$ relative to the references are shown on the left in Fig. 5, and at the right the corrections with $n_+ < n_-$ are presented. To take circular birefringence into account we used $(n_{1+}, n_{2+}, n_{3+}) = (1.3800, 1.4000, 1.4300)$ and $(n_{1-}, n_{2-}, n_{3-}) = (1.3803, 1.4004, 1.4306)$ in the left column and $(n_{1+}, n_{2+}, n_{3+}) = (1.3800, 1.4000, 1.4300)$ and $(n_{1-}, n_{2-}, n_{3-}) = (1.3797, 1.3996, 1.4294)$ in the right column of Fig. 5. We found that a nonvanishing s-polarized signal can emerge from an sp input polarization combination when the circular birefringence effect is included, which indicates that circular birefringence causes the nonlinear polarization to point away from the plane of incidence. In addition, circular birefringence leads to a slight increase in the p-polarized SFG intensity with $n_+ > n_-$ and to a decrease with $n_+ < n_-$.

In a surface sum-frequency measurement, an azimuthally isotropic polar layer with an effective surface susceptibility of $\chi_s^{(2)}$ can generate only an s-polarized SFG signal by use of an sp input polarization combination.[24,25] Based on our analysis of the bulk contribution from a chiral liquid, both the sp and the ps polarization combinations produce a p-polarized sum-frequency field when the circular birefringence effect is neglected. From the s-polarized intensity variations shown in Figs. 5(a) and 5(b) and the p-polarized intensity reference [the dotted curve in Fig. 4(a)] we can deduce that $\Delta I_{3rs}/I_{3rp} \approx 10^{-7}$. Looking at the dotted curves in Figs. 4(a) and 4(b), we can observe that the peak value of the transmitted SFG intensity is approximately ten times larger than that of the reflected SFG intensity. This finding indicates that the effective nonlinear susceptibility for reflected SFG, $\chi_{\mathrm{eff},r}^{(2)}$, is approximately three tenths of that for the transmitted SFG, $\chi_{\mathrm{eff},t}^{(2)}$. Inasmuch as $\chi_{\mathrm{eff},t}^{(2)}$ for a 2.46-M solution of arabinose was measured to be $\sim 1 \times 10^{-10}$ esu,[16] $\chi_{\mathrm{eff},r}^{(2)}$ can be estimated to be 3×10^{-11} esu. For a solution of arabinose, the value of $|\chi_s^{(2)}/(\chi_{\mathrm{eff},r}^{(2)} l_c)|^2$ was therefore found to be $\sim 10^{-3}$, which is much larger than $\Delta I_{3rs}/I_{3rp}$. This result implies that the nonvanishing s-polarized sum-frequency signal caused by the circular birefringence effect of a chiral medium is negligible compared with the surface contribution. One can therefore distinguish the surface signal from the bulk contribution by measuring the s-polarized SFG signal for the surface contribution and the p-polarized SFG signal for the bulk contribution by using either sp or ps as the input polarization combination.

B. Spectroscopic Applications

Although electronic CD spectroscopy was developed at the end of last century, the first vibrational CD[26,27] was not demonstrated until the 1970's. During the past few decades, vibrational CD had been rigorously developed into a useful tool for probing chirality with molecular specificity. From a theoretical point of view, a vibrational wave function is better understood and is easier to calculate than an electronic wave function. Therefore structural information will be more reliably extracted from a measured vibrational spectrum through a careful comparison with theoretical calculation. Vibrational spectra from an intramolecular functional group have been shown to be highly sensitive to the perturbation from a nearby chiral center.[28,29] Therefore a sum-frequency process that combines an optical photon and a frequency-tunable infrared photon is a promising tool for studying chirality-induced phenomena.[30]

In an infrared-visible SFG experiment one can investigate the resonant behavior of $\chi_a^{(2)}$ by tuning the incident infrared beam across some vibrational resonance of a chiral molecule. Unlike linear optical CD, for which one needs to extract a small differential signal from a large background because of the weak coupling between the magnetic and the electric transition dipole moments,[26,27] SFG spectroscopy as discussed above is purely electric-dipole contributed and background free. Furthermore, the SFG spectroscopic characterization of $\chi_a^{(2)}$ can offer valuable information about the substructure of a chiral molecule.

The chirality specificity of our proposed spectroscopic technique can facilitate the study of solvation processes. For an accurate measurement of molecular nonlinear optical properties in condensed phase the solute–solvent interaction must be carefully taken into account. Unfortunately, the solvation processes[31] of a molecule are not well understood. As far as a second-order nonlinear optical process is concerned, an ordered polar structure is needed and the resulting nonlinear optical signal depends on the order of the orientational distribution. To investigate the influence of the surrounding solvent on the nonlinear optical response of the solute molecules we must first have a clear picture of the molecular orientational distribution. Chiral molecules can serve as useful probes for studying the solvent effect because the totally antisymmetric part of second-order susceptibility is sensitive only to molecular chirality. Thus the resulting SFG signal will originate purely from the chiral solute if the solvent is achiral. Furthermore, note from Eq. (18) that the totally antisymmetric part, which is rotationally invariant under rotational operation, permits a fairly straightforward connection of $\chi_a^{(2)} = N\alpha_a^{(2)}$ between the macroscopic nonlinear susceptibility $\chi^{(2)}$ and the microscopic nonlinear molecular polarizability $\alpha^{(2)}$. Thus the nonlinear molecular polarizability can easily be determined from the measured nonlinear susceptibility. The solvent effect may be also reflected in a relative peak shift or a magnitude change in the spectra of chiral molecules in different solvents. The quadrupole contribution from the achiral solvent may mask these chirality-induced signals in a dilute solution. The SFG amplitude ratio of the quadrupole to the dipole contribution can be roughly estimated from the spatial dispersion parameter a/λ, where a is the characteristic dimension of the molecules and λ is the wavelength. In the visible range, a/λ is 10^{-2}–10^{-4}. To avoid the masking effect from the solvent's quadrupole contribution, the volume fraction of the chiral solute must exceed 10^{-2}.

4. SUMMARY

We have solved the problem of the nonlinear reflection and transmission for sum-frequency generation from the bulk of a chiral liquid. The dependence of the SFG intensity on the incident angles and the polarizations of two incident beams was analyzed. The optimal experimental arrangement that gives the strongest SFG signal has been discovered. We also included the circular birefringence effect of a chiral medium in our formalism. Our calculations showed that the circular birefringence of a chiral medium makes only a small correction to the SFG intensity. The potential of chirality-induced SFG in spectroscopic applications was also assessed and discussed.

APPENDIX A: FRESNEL COEFFICIENTS

Owing to the appearance of circular birefringence in a chiral medium, the beam refracted into the medium will split into a LHCP and a RHCP wave. Because the eigenwaves in a chiral medium are circularly polarized, we can not separately describe the reflection and the transmission of s- and p-polarized waves. To determine the amplitude of a refracted wave, we first decompose the incident and the reflected electric fields into s and p components, E_{is}, E_{ip}, E_{rs}, and E_{rp}, and then decompose the refracted wave into LHCP and RHCP components, E_{t+} and E_{t-}. The same decomposition is also applied to the magnetic fields. Continuity of the tangential components of electric fields across a planar boundary yields the following two equations:

$$E_{is} + E_{rs} = \frac{1}{\sqrt{2}}(E_{t+} + E_{t-}),$$

$$-E_{ip}\cos\theta_i + E_{rp}\cos\theta_r = \frac{i}{\sqrt{2}}(-E_{t+}\cos\theta_{t+} + E_{t-}\cos\theta_{t-}). \tag{A1}$$

Continuity of the tangential components of magnetic fields across the boundary provides two additional equations:

$$H_{is} + H_{rs} = \frac{1}{\sqrt{2}}(H_{t+} + H_{t-}),$$

$$-H_{ip}\cos\theta_i + H_{rp}\cos\theta_r = \frac{i}{\sqrt{2}}(-H_{t+}\cos\theta_{t+} + H_{t-}\cos\theta_{t-}). \tag{A2}$$

The electric and magnetic fields are connected by means of the following equations:

$$H_{is} = -\frac{c}{\mu_0\omega}k_i E_{ip}, \qquad H_{ip} = \frac{c}{\mu_0\omega}k_i E_{is},$$

$$H_{rs} = -\frac{c}{\mu_0\omega}k_r E_{rp}, \qquad H_{rp} = \frac{c}{\mu_0\omega}k_r E_{rs},$$

$$H_{t+} = -\frac{c}{\mu\omega}ik_{t+}E_{t+}, \qquad H_{t-} = \frac{c}{\mu\omega}ik_{t-}E_{t-}. \tag{A3}$$

For nonmagnetic media for which $\mu = \mu_0$, Eqs. (A1) and (A2) can be solved to yield the following matrix equation:

$$\begin{bmatrix} 1 & 0 & \frac{-1}{\sqrt{2}} & \frac{-1}{\sqrt{2}} \\ 0 & \cos\theta_r & \frac{i}{\sqrt{2}}\cos\theta_{t+} & \frac{-i}{\sqrt{2}}\cos\theta_{t-} \\ 0 & -k_r & \frac{i}{\sqrt{2}}k_{t+} & \frac{-i}{\sqrt{2}}k_{t-} \\ k_r\cos\theta_r & 0 & \frac{1}{\sqrt{2}}k_{t+}\cos\theta_{t+} & \frac{1}{\sqrt{2}}k_{t-}\cos\theta_{t-} \end{bmatrix} \times \begin{bmatrix} E_{rs} \\ E_{rp} \\ E_{t+} \\ E_{t-} \end{bmatrix} = \begin{bmatrix} -E_{is} \\ E_{ip}\cos\theta_i \\ k_i E_{ip} \\ k_i E_{is}\cos\theta_i \end{bmatrix}. \tag{A4}$$

By solving Eq. (A4) we can express E_{rs} and E_{rp} in terms of E_{is} and E_{ip}:

$$\begin{bmatrix} E_{rs} \\ E_{rp} \end{bmatrix} = \begin{bmatrix} r_{11} & r_{12} \\ r_{21} & r_{22} \end{bmatrix}\begin{bmatrix} E_{is} \\ E_{ip} \end{bmatrix}, \tag{A5}$$

$$\begin{bmatrix} E_{t+} \\ E_{t-} \end{bmatrix} = \begin{bmatrix} t_{11} & t_{12} \\ t_{21} & t_{22} \end{bmatrix}\begin{bmatrix} E_{is} \\ E_{ip} \end{bmatrix}. \tag{A6}$$

The matrix elements have been determined to be

$$t_{11} = \frac{\sqrt{2}}{D}(n_-\cos\theta_i + \cos\theta_{t-})2\cos\theta_i,$$

$$t_{12} = \frac{-i\sqrt{2}}{D}(n_-\cos\theta_{t-} + \cos\theta_i)2\cos\theta_i,$$

$$t_{21} = \frac{\sqrt{2}}{D}(n_+\cos\theta_i + \cos\theta_{t+})2\cos\theta_i,$$

$$t_{22} = \frac{i\sqrt{2}}{D}(n_+\cos\theta_{t+} + \cos\theta_i)2\cos\theta_i;$$

$$r_{11} = \frac{-1}{D}[(n_+n_- - 1)(\cos\theta_{t+} + \cos\theta_{t-})\cos\theta_i - (n_+ + n_-)(\cos^2\theta_i - \cos\theta_{t+}\cos\theta_{t-})],$$

$$r_{12} = \frac{2i}{D}(n_+\cos\theta_{t+} - n_-\cos\theta_{t-})\cos\theta_i,$$

$$r_{21} = \frac{-2i}{D}(n_-\cos\theta_{t+} - n_+\cos\theta_{t-})\cos\theta_i,$$

$$r_{22} = \frac{1}{D}[(n_+n_- - 1)(\cos\theta_{t+} + \cos\theta_{t-})\cos\theta_i + (n_+ + n_-)(\cos^2\theta_i - \cos\theta_{t+}\cos\theta_{t-})], \tag{A7}$$

where

$$D \equiv (n_+ n_- + 1)(\cos\theta_{t+} + \cos\theta_{t-})\cos\theta_i + (n_+ + n_-) \times (\cos^2\theta_i + \cos\theta_{t+}\cos\theta_{t-}). \quad \text{(A8)}$$

ACKNOWLEDGMENTS

The authors are indebted to K. J. Song for his helpful suggestions and stimulating discussions. We also appreciate financial support from the National Science Council of the Republic of China under grant NSC86-2112-M009-018.

Address any correspondence to J. Y. Huang.

REFERENCES

1. I. Gutman, V. Babovic, and S. Jokic, "The origin of biomolecular chirality: the generalized Frank model with arbitrary initial conditions," Chem. Phys. Lett. **144**, 187–190 (1988).
2. See, for example, A. W. Hall, J. Hollingshurst, and J. W. Goodby, "Chiral and achiral calamitic liquid crystals for display applications," in *Handbook of Liquid Crystal Research*, P. J. Collings and J. S. Patel, eds. (Oxford U. Press, Oxford, 1997), Chap. 2.
3. E. U. Condon, "Theories of optical rotatory power," Rev. Mod. Phys. **9**, 432–457 (1937).
4. J. D. Byers, H. I. Yee, and J. M. Hicks, "A second harmonic generation analog of optical rotatory dispersion for the study of chiral monolayers," J. Chem. Phys. **101**, 6233–6241 (1994).
5. T. Petralli-Mallow, T. M. Wong, J. D. Byers, H. I. Yee, and J. M. Hicks, "Circular dichroism spectroscopy at interfaces: a surface second harmonic generation study," J. Phys. Chem. **97**, 1383–1388 (1993).
6. J. D. Byers, H. I. Yee, T. Petralli-Mallow, and J. M. Hicks, "Second-harmonic generation circular-dichroism spectroscopy from chiral monolayers," Phys. Rev. B **49**, 14,643–16,647 (1994).
7. J. D. Byers and J. M. Hicks, "Electronic spectral effects on chiral surface second harmonic generation," Chem. Phys. Lett. **231**, 216–224 (1994).
8. J. M. Hicks, T. Petralli-Mallow, and J. D. Byers, "Consequences of chirality in second-order non-linear spectroscopy at surfaces," Discuss. Faraday Soc. **99**, 341–357 (1994).
9. T. Verbiest, M. Kauranen, J. J. Maki, M. N. Teerenstra, A. J. Schouten, R. J. M. Nolte, and A. Persoons, "Linearly polarized probes of surface chirality," J. Chem. Phys. **103**, 8296–8298 (1995).
10. J. J. Maki, T. Verbiest, M. Kaurenen, S. V. Elshocht, and A. Persoons, "Comparison of linearly and circularly polarized probes of second-order optical activity of chiral surfaces," J. Chem. Phys. **105**, 767–772 (1996).
11. Y. R. Shen, *The Principles of Nonlinear Optics* (Wiley, New York, 1984), Chap. 6.
12. K. B. Eisenthal, "Equilibrium and dynamic processes at interfaces by second harmonic and sum frequency generation," Annu. Rev. Phys. Chem. **43**, 627–661 (1992).
13. J. Y. Huang and Y. R. Shen, "Sum-frequency generation as a surface probe," in *Laser Spectroscopy and Photochemistry on Metal Surfaces*, H. L. Dai and W. Ho, eds. (World Scientific, Singapore, 1995), Vol. 1, pp. 5–53.
14. See, for example, G. Arfken, *Mathematical Methods for Physicists* (Academic, Orlando, Fla., 1985), Chap. 3.
15. J. A. Giordmaine, "Nonlinear optical properties of liquids," Phys. Rev. A **138**, 1599–1606 (1965).
16. P. M. Rentzepis, J. A. Giordmaine, and K. W. Wecht, "Coherent optical mixing in optically active liquids," Phys. Rev. Lett. **16**, 762–794 (1966).
17. D. A. Kleinman, "Nonlinear dielectric polarization in optical media," Phys. Rev. **126**, 1977–1979 (1962).
18. S. N. Volkov, N. I. Koroteev, and V. A. Makarov, "Sum-frequency generation by reflection of light from the surface of a nonabsorbing isotropic and gyrotropic medium," Quantum Electron. **25**, 1183–1187 (1995).
19. N. I. Koroteev, V. A. Makarov, and S. N. Volkov, "Sum frequency generation by reflection of light from the surface of a chiral medium," Nonlinear Opt. **17**, 247–269 (1997).
20. P. Pelet, and N. Engheta, "The theory of chirowaveguides," IEEE Trans. Antennas Propag. **38**, 90–98 (1990).
21. S. Bassiri, C. H. Papas, and N. Engheta, "Electromagnetic wave propagation through a dielectric-chiral interface and through a chiral slab," J. Opt. Soc. Am. A **5**, 1450–1459 (1988).
22. Y. R. Shen, *The Principles of Nonlinear Optics* (Wiley, New York, 1984), Chap. 2.
23. J. F. Nicoud and R. J. Twieg, "Organic EFISH hyperpolarizability data," in *Nonlinear Optical Properties of Organic Molecules and Crystals*, D. S. Chemla and J. Zyss, eds. (Academic, Orlando, Fla., 1987), Vol. 2, pp. 255–267.
24. Q. Du, R. Superfine, E. Freysz, and Y. R. Shen, "Vibrational spectroscopy of water at the vapor/water interface," Phys. Rev. Lett. **70**, 2313–2316 (1993).
25. C. D. Stanners, Q. Du, R. P. Chin, P. Cremer, G. A. Somorjai, Y.-R. Shen, "Polar ordering at the liquid-vapor interface of n-alcohols (C_1–C_8)," Chem. Phys. Lett. **232**, 407–413 (1995).
26. P. J. Stephens and M. A. Lowe, "Vibrational circular dichroism," Annu. Rev. Phys. Chem. **36**, 213–241 (1985).
27. T. B. Freedman and L. A. Nafie, "Stereochemical aspects of vibrational optical activity," in *Topics in Stereochemistry*, E. Eliel and S. Wilen, eds. (Wiley, New York, 1987), pp. 113–206.
28. D. Barron, "Methyl group as a probe of chirality in Raman optical activity," Nature (London) **255**, 458–460 (1975).
29. M. Diem, E. Photos, H. Khouri, and L. A. Nafie, "Vibrational circular dichroism in amino acids and peptides: 3. Solution- and solid-phase spectra of alanine and serine," J. Am. Chem. Soc. **101**, 6829–6837 (1979).
30. N. I. Koroteev, "New schemes for nonlinear optical spectroscopy of solutions of chiral biological macromolecules," JETP **79**, 681–690 (1994).
31. J. L. Finney, "Hydration processes in biological and macromolucular systems," Discuss. Faraday Soc. **103**, 1–18 (1996).